Inventory of Supplemental Information: Cerniauskas et al.

Supplementary Figures:

Supplementary Table:

Supplemental Material: Cerniauskas et al.

Figure S1. Analysis of chronic stress-induced behavioral phenotypes, Related to Figure 1.

(A) Schematic showing C57BL/6 mice in the tail suspension test (TST) and one week later in the forced swim test (FST).

(B) Correlation of struggling behavior between TST and FST for CTRL (green) and CMS (blue) mice (CTRL: n = 13 mice, $R^2 = 0.51$, p = 0.006; CMS: n = 14 mice, $R^2 = 0.43$, p = 0.011; linear correlations).

(C) Schematic of experimental design. Session 1 evaluates the social interaction behavior between a subject and an unfamiliar mouse (Stranger 1). Session 2 evaluates the interest of a subject in social novelty by introducing another unfamiliar mouse (Stranger 2).

(D) Graphs showing measures of sociability (left; CTRL: 1.97 ± 0.2, n = 20 mice, CMS: 2.45 ± 0.2, n = 37 mice; p = 0.1, unpaired Student's t-test) and social novelty (right; CTRL: 1.5 ± 0.2, n = 20 mice, CMS: 1.54 ± 0.2, n = 37 mice; p = 0.86, unpaired Student's t-test) for CTRL and CMS mice (data represent means ± SEM).

(E) Left bar graphs shows time spent in open arms for C57BL/6 mice tested in the elevated plus maze (EPM) for the 1st time (1st run) and then re-tested two weeks later (2nd run) (1st run: 201.8 ± 14.3 s, n = 14 mice; 2nd run: 108.0 ± 15.7 s, n = 14 mice; p < 0.001, paired Student's t-test). Right bar graph shows linear correlation between 1st run and 2nd run for time spent in open arms for individual mice (n = 14 mice, $R^2 = 0.39$, p = 0.018; linear correlation).

(F) Left bar graphs shows sucrose consumption for C57BL/6 mice tested in the sucrose preference test (SPT) for the 1st time (1st run) and then re-tested two weeks later (2nd run) (1st run: 69.2 ± 3.4 %, n = 23 mice; 2nd run: 71.4 ± 3.4 %, n = 23 mice; p = 0.53, paired Student's t-test). Right bar graph shows linear correlation between 1st run and 2nd run for sucrose consumption for individual mice (n = 23 mice, $R^2 = 0.23$, p = 0.022; linear correlation).

(G) Left bar graphs shows time spent struggling for C57BL/6 mice tested in TST for the 1st time (1st run) and then re-tested two weeks later (2nd run) (1st run: 119.6 ± 7.3 s, n = 14 mice; 2nd run: 74.9 ± 7.0 s, n = 14 mice; p < 0.001, paired Student's t-test). Right bar graph shows linear correlation between 1st run and 2nd run for struggling time for individual mice (n = 14 mice, $R^2 = 0.53$, p = 0.003; linear correlation).

Figure S2. Bootstrapping suggests that experimentally-determined cutoff values and D-score subgroups are stable representations, Related to Figure 1.

Based on the large sample sizes used to determine cutoff values in **Figures 1A-1C** (EPM: n = 100 mice; SPT: n = 145 mice; TST = 163 mice), we assumed that these samplings are appropriate representations of real CTRL and CMS distributions for EPM, SPT and TST behavioral tests. First, we sampled with replacement from our experimental data 10,000 times. For example, we drew 43 samples (original experimental sample size) with replacement from TST CTRL group and 120 samples (same reason) from TST CMS group. Then we applied ROC curves to determine a cutoff value from this subsample. Repeating this procedure 10,000 times gave us bootstrapped distributions of cutoff values for anxiety, anhedonia and immobility shown in **Figure S2A**. We observed that our experimentally determined cutoff values were very close to median cutoff values from bootstrapped distributions (EPM: 181.9 s versus 181.9 s; SPT: 60.1% versus 63.2%; TST: 93.5 s versus 95.5 s). Second, we applied our bootstrapped cutoff values to our experimental CTRL and CMS populations from Figures 1E and 1F. For example, we applied one set of bootstrapped EPM, SPT and TST cutoff values to CTRL and CMS mice from Figures 1E and 1F and classified those mice to D-score categories accordingly. After repeating this procedure 10,000 times, we had distributions of D-scores for CTRL and CMS mice (**Figures S2B-S2E**). After comparing our experimentally-determined D-score distributions (**Figures 1G and 1H**) with median bootstrapped D-score distribution values, we again saw close correspondence between the two (CTRL D0: 36.2% versus 25.6%, CTRL D1: 37.7% versus 38.5%, CTRL D2: 23.2% versus 30.8%, CTRL D3: 2.9% versus 2.6%; CMS D0: 5.6% versus 3.1 %, CMS D1: 28.0% versus 20.3%, CMS D2: 47.7% versus 43.8%, CMS D3: 18.7% versus 29.7%).

Figure S3. Comparison of LHb→VTA and LHb→DR subpopulations, Related to Figure 2.

(A) Schematic of experimental design showing dual retrograde tracing of LHb→VTA (red beads) and LHb→DR (green beads) subpopulations.

(B) Sample confocal image showing no overlap between retrogradely labeled LHb→VTA (green arrows) and LHb→DR (red arrows) cells in the LHb (DAPI: blue; Scale bar: 20 μm)

(C) Bar graph showing that the majority of retrogradely labeled cells harbor either red or green fluorescent beads and only a small portion of cells contains both red and green beads (VTA or

DR: 94.2 ± 1.9 % (620/654 cells), VTA and DR co-labeled: 5.8 ± 1.9 % (34/654 cells), n = 3 mice; data represent means ± SEM). Inset shows sample confocal image of a cell that is co-labeled with red and green beads.

(D) Schematic of experimental design showing retrograde tracing of LHb→VTA neurons by injection of a glycoprotein-deleted rabies virus expressing GFP into the VTA.

(E) Fluorescent image showing retrogradely labeled (RV-GFP, green) LHb→VTA cells in the lateral part of the LHb (DAPI: blue, MHb: medial habenula, 3V: 3rd ventricle; Scale bar: 200 μm).

(F) Schematic of experimental design showing retrograde tracing of LHb→DR neurons by injection of a glycoprotein-deleted rabies virus expressing GFP into the DR.

(G) Fluorescent image showing retrogradely labeled (RV-GFP, green) LHb→DR cells in the medial part of the LHb (DAPI: blue, MHb: medial habenula, 3V: 3rd ventricle; Scale bar: 200 μm).

(H) Schematic of experimental design showing injection of an AAV expressing ChR2 (using CaMKII promoter) into the LHb and optogenetic stimulation of excitatory LHb terminals in the VTA.

(I) Trajectory of a typical animal that received 10 Hz light stimulation of LHb terminals in the VTA in one compartment (Phase 1, blue, top panel) for the initial 10 min period followed by stimulation in the other compartment (Phase 2, blue, lower panel) for an additional 10 min.

(J) Time spent in individual compartments (non-stimulated side: black; stimulated side: blue) plotted as a function of time over the course of the experiment (1 min intervals) for LHb terminal stimulation in the VTA. Dashed line indicates switching of compartment stimulation after 10 min (data represent means ± SEM).

(K) Bar graph showing total time spent in stimulated and non-stimulated compartments for light stimulation of LHb terminals in the VTA (Stim.: 282.2 ± 35.6 s, Non-stim: 592.3 ± 43.8 s, n = 8 mice; *** $p < 0.001$, unpaired Student's t-test, data represent means ± SEM).

(L) Schematic of experimental design showing injection of an AAV expressing ChR2 (using CaMKII promoter) into the LHb and optogenetic stimulation of excitatory LHb terminals in the DR.

(M) Trajectory of a typical animal that received 10 Hz light stimulation of LHb terminals in the

DR in one compartment (Phase 1, blue, top panel) for the initial 10 min period followed by stimulation in the other compartment (Phase 2, blue, lower panel) for an additional 10 min.
(N) Time spent in individual compartments (non-stimulated side: black; stimulated side: blue) plotted as a function of time over the course of the experiment (1 min intervals) for LHb terminal stimulation in the DR. Dashed line indicates switching of compartment stimulation after 10 min (data represent means ± SEM).
(O) Bar graph showing total time spent in stimulated and non-stimulated compartments for light stimulation of LHb terminals in the DR (Stim.: 344.9 ± 30.1 s, Non-stim: 536.2 ± 34 s, n = 7 mice; ** $p < 0.01$, unpaired Student's t-test, data represent means ± SEM).
(P) Statistical comparison of evoked firing in LHb→VTA neurons for CMS_{D2} and $CTRL_{D2}$ versus $CTRL_{D0\text{-}1}$ and $CMS_{D0\text{-}1}$ mice. LHb→VTA neurons in CMS_{D2} mice showed significantly increased evoked firing when compared to $CTRL_{D0\text{-}1}$ and $CMS_{D0\text{-}1}$ mice. On average, $CTRL_{D2}$ mice showed higher evoked firing rates compared to $CTRL_{D0\text{-}1}$ mice. However, there was no statistically significant difference for comparison of $CTRL_{D2}$ versus CMS_{D2}, $CMS_{D0\text{-}1}$ or $CTRL_{D0\text{-}1}$ mice. Evoked firing rates in response to +150 pA current injections: $CTRL_{D0\text{-}1}$: 37.4 ± 3.9 spikes, n = 37 cells; CMS_{D2}: 60.5 ± 4.8 spikes, n = 26 cells; $CMS_{D0\text{-}1}$: 32.3 ± 3.9 spikes, n = 29 cells; $CTRL_{D2}$: 41.1 ± 9.7 spikes, n = 14 cells; $CTRL_{D0\text{-}1}$ versus CMS_{D2} $p = 0.006$, $CMS_{D0\text{-}1}$ versus CMS_{D2} $p = 0.001$, $CTRL_{D2}$ versus CMS_{D2} $p = 0.14$, $CTRL_{D2}$ versus $CTRL_{D0}$ $p = 0.97$; one-way ANOVA $p = 0.001$, Tukey's post hoc test.
(Q) Bar graphs showing mean membrane resistances (left) and mean capacitances (right) for LHb→VTA and LHb→DR cells (membrane resistance: LHb→VTA: 391.2 ± 26.7 MOhm, n = 27 cells (11 mice), LHb→DR: 442.2 ± 41.6 MOhm, n = 11 cells (3 mice); $p = 0.31$; membrane capacitance: LHb→VTA: 20.3 ± 0.9 pF, n = 49 cells (11 mice), LHb→DR: 22.1 ± 1.3 pF, n = 14 cells (3 mice); $p = 0.36$; unpaired Student's t-tests; data represent means ± SEM).
(R) Bar graphs showing mean membrane resistances (left) and mean capacitances (right) in LHb→VTA neurons from $CTRL_{D0\text{-}1}$ and $CMS_{D2\text{-}3}$ mice (membrane resistance: $CTRL_{D0\text{-}1}$: 391.2 ± 26.7 MOhm, n = 27 cells (11 mice), $CMS_{D2\text{-}3}$: 456.8 ± 27.6 MOhm, n = 19 cells (9 mice); $p = 0.1$; membrane capacitance: $CTRL_{D0\text{-}1}$: 20.3 ± 0.9 pF, n = 49 cells (11 mice), $CMS_{D2\text{-}3}$: 22.9 ± 1.2 pF, n = 32 cells (9 mice); $p = 0.09$; unpaired Student's t-tests; data represent means ± SEM).

Figure S4. *In vivo* electrophysiology of LHb→VTA neurons, Related to Figure 3.

(A) 3D plot showing samples of three concurrently-recorded units that are plotted according to their action potential height; different colors indicate action potentials that belong to different units.

(B) Top: spike raster plots showing unit firing 50 ms before and 100 ms after the 5 ms laser pulse with each row representing one stimulation trial. The blue line indicates the start of the laser pulse. Bottom: corresponding spike histograms. Cell labeling corresponds to the color scheme in panel A (data represent means ± SEM).

(C) Isolated unit and its spontaneous (orange) and light evoked (blue) action potentials shown across different electrode pairs and plotted according to the action potential height.

(D) Isolated unit and its spontaneous (orange) and light evoked (blue) action potential shapes shown across different electrodes (Scale bar: 30 μV/0.5 ms).

(E) Histogram (blue) showing the distribution (orange) of number of spikes in the most active 2 ms bin for the shuffled data with the 99.9^{th} percentile indicated by an orange vertical line. The number of spikes in the most active 2 ms bin for the observed data is indicated by vertical purple line. See methods for further details.

(F) Graph showing mean response latency to laser stimulation for ChR2-tagged LHb→VTA neurons in $CTRL_{D0\text{-}1}$ (green) and $CMS_{D2\text{-}3}$ (blue) mice (4.79 ± 0.25 ms, n = 12 cells (6 mice); data represent means ± SEM).

(G) Top: spontaneous spike raster plots from $CTRL_{D0\text{-}1}$ (left) and $CMS_{D2\text{-}3}$ (right) mice. Bottom: spikes identified by rank surprise burst detection algorithm that belong to a burst are highlighted in orange (Scale bars: 500 ms).

(H) Mean percentage of spikes in bursts in non-labeled LHb cells from $CTRL_{D0\text{-}1}$ and $CMS_{D2\text{-}3}$ mice ($CTRL_{D0\text{-}1}$: 27.4 ± 0.8 %, n = 10 cells (3 mice), $CMS_{D2\text{-}3}$: 28.3 ± 1 %, n = 9 cells (3 mice); p = 0.5, unpaired Student's t-test; data represent means ± SEM).

(I) Mean number of spikes per burst in non-labeled LHb cells from $CTRL_{D0\text{-}1}$ and $CMS_{D2\text{-}3}$ mice ($CTRL_{D0\text{-}1}$: 4.4 ± 0.2 spikes, n = 10 cells (3 mice), $CMS_{D2\text{-}3}$: 5.1 ± 0.4 spikes, n = 9 cells (3 mice); p = 0.11, unpaired Student's t-test; data represent means ± SEM).

(J) Mean interburst frequencies in non-labeled LHb cells from $CTRL_{D0\text{-}1}$ and $CMS_{D2\text{-}3}$ mice ($CTRL_{D0\text{-}1}$: 0.77 ± 0.1 Hz, n = 10 cells (3 mice), $CMS_{D2\text{-}3}$: 0.7 ± 0.1 Hz, n = 9 cells (3 mice); p = 0.6, unpaired Student's t-test; data represent means ± SEM).

(K) Mean intraburst frequencies in non-labeled LHb cells from $CTRL_{D0-1}$ and CMS_{D2-3} mice ($CTRL_{D0-1}$: 205.3 ± 18.1 Hz, n = 10 cells (3 mice), CMS_{D2-3}: 245 ± 64.8 Hz, n = 9 cells (3 mice); p = 0.54, unpaired Student's t-test; data represent means ± SEM).
(L) Mean tonic firing frequencies in non-labeled LHb cells from $CTRL_{D0-1}$ and CMS_{D2-3} mice ($CTRL_{D0-1}$: 8.5 ± 1.3 Hz, n = 10 cells (3 mice), CMS_{D2-3}: 8.55 ± 1.1 Hz, n = 9 cells (3 mice); p = 0.98, unpaired Student's t-test; data represent means ± SEM).
(M) Mean firing frequencies in non-labeled LHb cells from $CTRL_{D0-1}$ and CMS_{D2-3} mice ($CTRL_{D0-1}$: 11.9 ± 1.9 Hz, n = 10 cells (3 mice), CMS_{D2-3}: 12 ± 1.6 Hz, n = 9 cells (3 mice); p = 0.96, unpaired Student's t-test; data represent means ± SEM).

Figure S5. Mapping of monosynaptic inputs to LHb→VTA and LHb→DR neurons, Related to Figure 4.

(A) Representative samples showing injection-site of CAV2-Cre (red) in the VTA (left) or DR (right) (DAPI: blue; IP: interpeduncular nucleus, AQ: cerebral aqueduct; Scale bars: 450 μm).
(B) Left: Confocal image showing the anatomical distribution of starter cells in the LHb for mapping inputs to LHb→DR neurons. Starter cells are defined as cells that co-express RV-GFP (green) and TVA-mCherry (red; Scale bar: 150 μm). Right: Higher magnification confocal image of the region highlighted in the left image (DAPI: blue; Scale bar: 60 μm).
(C) Percentage of the cells that are either TVA-mCherry positive or RV-GFP positive or cells that co-express TVA-mCherry and RV-GFP in the LHb for mapping of inputs to LHb→VTA (blue; n = 2 mice) and LHb→DR (green; n = 2 mice) neurons (TVA-mCherry-positive: LHb→VTA: 1.28 ± 0.4 %, LHb→DR: 1.18 ± 0.4 %, p = 0.99; RV-GFP-positive: LHb→VTA: 9.74 ± 0.9 %, LHb→DR: 22.98 ± 0.6 %, *** p < 0.001; TVA-mCherry and RV-GFP co-expression: LHb→VTA: 88.98 ± 0.5 %, LHb→DR TVA+/RV+: 75.84 ± 1 %, *** p < 0.001; two-way ANOVA interaction p < 0.001, Sidak's post hoc test; data represent means ± SEM).

Abbreviations used in **Figure 4D**: PFC: prefrontral cortex, ACC: anterior cingulate cortex, STR: striatum, EP: entopeduncular nucleus, PALc: caudal pallidum, PALm: medial pallidum, PALv: ventral pallidum, LSX: lateral septal complex, LPO: lateral preoptic area, PVX: paraventricular hypothalamic nucleus, LH: lateral hypothalamus, MEZ: hypothalamic medial zone, other HY: other hypothalamic areas, DORpm: polymodal association cortex related thalamus, other MB:

other midbrain, VTA: ventral tegmental area, SN: substantia nigra, MRN: median raphe nucleus, DR: dorsal raphe nucleus, PAG: periaqueductal gray, SC: superior colliculus.

Figure S6. Role of LHb→VTA and EP→LHb neurons in passive coping and effort-related motivated behavior, Related to Figure 6.

(A) Left: Schematic of experimental design showing optogenetic stimulation of LHb→VTA neurons in non-stressed mice. Right: Coronal brain section showing ChR2-eYFP (green) expression in a subset of LHb neurons projecting to VTA (3V: 3rd ventricle, MHb: medial habenula; DAPI: blue; Scale bar: 300 μm).

(B) Bar graphs showing time spent in open arms in EPM, sucrose consumption in SPT, time spent struggling in TST and total distance travelled in OFT for mice expressing eYFP or ChR2 in LHb→VTA neurons (EPM: eYFP: 134.4 ± 21 s, n = 10 mice, ChR2: 93.4 ± 12.7 s, n = 10 mice, p = 0.11; SPT: eYFP: 63.6 ± 8.9 %, n = 9 mice, ChR2: 65.6 ± 5.2 %, n = 9 mice, p = 0.85; TST: eYFP: 99.5 ± 6.9 s, n = 10 mice, ChR2: 70.7 ± 5.3 s, n = 10 mice, ** p = 0.004; OFT: eYFP: 2063 ± 170.8 cm, n = 10 mice, ChR2: 1731 ± 172 cm, n = 10 mice, p = 0.19; all unpaired Student's t-test; data represent means ± SEM).

(C) Left: Schematic of experimental design showing chemogenetic activation of LHb→VTA neurons in non-stressed mice. Middle: Coronal brain section showing hM3DGq-mCherry (red) expression in a subset of LHb neurons projecting to VTA (DAPI: blue; Scale bar: 200 μm). Right: Bar graphs showing time spent struggling in the forced swim test (FST) after CNO injections for mice expressing eYFP or hM3DGq-mCherry in LHb→VTA neurons (mCherry: 81.5 ± 6.8 s, n = 8 mice; hM3DGq: 55.1 ± 7.4 s, n = 7 mice; p = 0.021, unpaired Student's t-test; data represent means ± SEM).

(D) Left: Schematic of experimental design showing chemogenetic activation of EP→LHb neurons in non-stressed mice. Middle: Coronal brain section showing hM3DGq-mCherry (red) expression in a subset of EP neurons projecting to LHb (DAPI: blue; Scale bar: 200 μm). Right: Bar graphs showing time spent struggling in the FST after CNO injections for mice expressing eYFP or hM3DGq-mCherry in EP→LHb neurons (mCherry: 101.9 ± 9.0 s, n = 8 mice; hM3DGq: 74.3 ± 5.8 s, n = 7 mice; p = 0.026, unpaired Student's t-test; data represent means ± SEM).

(E) Number of nose pokes over time in fixed ratio operant behavior after saline (left) and CNO (middle) injections for mice expressing eYFP or hM3DGq in LHb→VTA neurons. Right: Graph showing total number of nose pokes for saline (black) and CNO (blue) injected eYFP and hM3DGq mice ($eYFP_{saline}$: 71.7 ± 6.3 pokes, $eYFP_{CNO}$: 72.4 ± 8.4 pokes, n = 14 mice, p = 0.94; $hM3DGq_{saline}$: 78.8± 8.8 pokes, $hM3DGq_{CNO}$: 59± 6.3 pokes, n = 13 mice, p = 0.09; two-way RM ANOVA, there was no saline / CNO effect (p = 0.16) and no eYFP / hM3DGq effect (p = 0.72), Holm-Sidak's post hoc test).

(F) Number of nose pokes over time in progressive ratio operant behavior after saline (left) and CNO (middle) injections for mice expressing eYFP or hM3DGq in LHb→VTA neurons. Right: Graph showing total number of nose pokes for saline (black) and CNO (blue) injected eYFP and hM3DGq mice ($eYFP_{saline}$: 912.3 ± 141.4 pokes, $eYFP_{CNO}$: 773.8 ± 153 pokes, n = 14 mice, p = 0.4; $hM3DGq_{saline}$: 686.5 ± 132.8 pokes, $hM3DGq_{CNO}$: 254.8± 37.6 pokes, n = 13 mice, * p = 0.035; two-way RM ANOVA, there was saline / CNO effect (p = 0.023) and eYFP / hM3DGq effect (p = 0.011), Holm-Sidak's post hoc test).

(G) Number of nose pokes over time in fixed ratio operant behavior after saline (left) and CNO (middle) injections in mice expressing eYFP or hM3DGq in EP→LHb neurons. Right: Graph showing total number of nose pokes for saline (black) and CNO (blue) injected eYFP and hM3DGq mice ($eYFP_{saline}$: 93.1 ± 6.4 pokes, $eYFP_{CNO}$: 95 ± 12.1 pokes, n = 9 mice, p = 0.92; $hM3DGq_{saline}$: 109 ± 17.4 pokes, $hM3DGq_{CNO}$: 92.2 ± 11.7 pokes, n = 9 mice, p = 0.58; two-way RM ANOVA, there was no saline / CNO effect (p = 0.56) and no eYFP / hM3DGq effect (p = 0.61), Holm-Sidak's post hoc test).

(H) Number of nose pokes over time in progressive ratio operant behavior after saline (left) and CNO (middle) injections in mice expressing eYFP or hM3DGq in EP→LHb neurons. Right: Bar graph showing total number of nose pokes for saline (black) and CNO (blue) injected eYFP and hM3DGq mice ($eYFP_{saline}$: 937 ± 182.4 pokes, $eYFP_{CNO}$: 815.4 ± 185.4 pokes, n = 9 mice, p = 0.58; $hM3DGq_{saline}$: 655.4 ± 102.8 pokes, $hM3DGq_{CNO}$: 743.3 ± 125.4 pokes, n = 9 mice, p = 0.58; two-way RM ANOVA, there was no saline / CNO effect (p = 0.85) and no eYFP / hM3DGq effect (p = 0.38), Holm-Sidak's post hoc test).

Figure S7. Molecular and physiological correlates of passive coping, Related to Figure 7.

(A) Schematic showing the anatomical location of TST- LHb→VTA (green), TST+ LHb→VTA

(blue) and TST- LHb→DR (brown) cells in the LHb (MHb: medial habenula, DG: dentate gyrus, 3V: 3rd ventricle, sm: stria medullaris, fr: fasciculus retroflexus).

(B) Mean number of action potentials in response to injection of a +150 pA depolarizing current in LHb→VTA neurons from mice that were pooled according to whether they were positive or negative for a specific behavioral phenotype (i.e. anxiety assessed in EPM (left), anhedonia assessed in SPT (right)). Animals were considered positive if they scored below the corresponding cutoff value defined in **Figures 1A-1C** (EPM: neg: 48.4 ± 5.9 spikes, n = 26 cells (5 mice), pos: 41.9 ± 3.2 spikes, n = 68 cells (11 mice), p = 0.32; SPT: neg: 43.4 ± 4 spikes, n = 44 cells (6 mice), pos: 41.8 ± 4.5 spikes, n = 43 cells (10 mice), p = 0.78; all unpaired Student's t-test).

(C) Graphs showing evoked number of action potentials in response to injection of a +150 pA depolarizing ramp current in LHb→VTA neurons and their correlation with time spent in open arms in EPM (left), sucrose consumed in SPT (middle) and time spent struggling in TST (right; EPM: $R^2 = 0.02$, p = 0.14, SPT: $R^2 = 0.27$, p = 0.01, TST: $R^2 = 0.02$, p = 0.04).

(D) Mean resting membrane potential recorded from cells that predominantly fire tonically or in bursts (Tonic: -50.1 ± 1.2 mV, n = 30 cells (14 mice), burst: -58.4 ± 0.5 mV, n = 78 cells (17 mice); *** $p < 0.001$, unpaired Student's t-test; data represent means ± SEM).

(E) Cumulative frequency of resting membrane potential recorded from cells that predominantly fire tonically (grey) or in bursts (black).

(F) Volcano plots show differential gene expression between single LHb→VTA (n = 16 cells, 5 mice) and LHb→DR neurons (n = 14 cells, 5 mice) in TST- mice. Gold and brown data points denote genes that are significantly enriched in TST- LHb→VTA versus TST- LHb→DR neurons, respectively. Highlighted are the cell adhesion molecule-coding (CAM; top left), ion channel-coding (top right), transcription factor-coding (bottom left) and synapse-related (bottom right) genes. Gray data points represent genes that are not significantly enriched in either category (i.e. absolute value of Log2(Fold Change) < 2 and $p < 0.01$).

(G) Volcano plots show differential gene expression between single LHb→VTA neurons in TST- (n = 16 cells, 5 mice) versus TST+ (n = 37 cells, 10 mice) mice. Green and blue data points denote genes that are significantly enriched in cells from TST- versus TST+ mice, respectively. Highlighted are the cell adhesion molecule-coding (CAM; top left), ion channel-coding (top right), transcription factor-coding (bottom left) and synapse-related (bottom right) genes. Gray

data points represent genes that are not significantly enriched in either category (i.e. absolute value of Log2(Fold Change) < 2 and p < 0.01).
(H) Violin plots show expression of *Ptprr* (top left), *Grik2* (top right), *Lrrtm3* (middle left), *Rundc1* (middle right), *Myt1l* (bottom left) and *Smim8* (bottom right) as examples from TST- (n = 16 cells, 5 mice) and TST+ LHb→VTA (n = 37 cells, 10 mice) and TST- LHb→DR (n = 14 cells, 5 mice) mice.

Figure S8. Single-cell transcriptomic analysis for comparison of CTRL and CMS mice, Related to Figure 7.

(A) Volcano plots displaying differential gene expression between single LHb→VTA (n = 26 cells, 9 mice) and LHb→DR (n = 18 cells, 6 mice) neurons in CTRL mice. Gold and brown data points denote genes that are significantly enriched in LHb→VTA versus LHb→DR neurons from CTRL mice, respectively. Highlighted in black are the ion channel-coding and synapse-related genes. Highlighted in red are the genes that are detected as significantly differently expressed in LHb→VTA versus LHb→DR neurons from TST- but not from CTRL mice (see **Figure 7**). Gray data points represent genes that are not significantly enriched in either category (i.e. absolute value of Log2(Fold Change) < 2 and p < 0.01).
(B) Violin plot displaying differential gene expression between single LHb→VTA neurons in CTRL (n = 26 cells, 9 mice) versus CMS (n = 27 cells, 6 mice) mice. Green and blue data points denote genes that are significantly enriched in cells from CTRL versus CMS mice, respectively. Highlighted in black are the ion channel-coding and synapse-related genes. Highlighted in red are the genes that are detected as significantly differently expressed in LHb→VTA versus LHb→DR neurons from TST- but not from CTRL mice (see **Figure 7**). Gray data points represent genes that are not significantly enriched in either category (i.e. absolute value of Log2(Fold Change) < 2 and p < 0.01).
(C) Violin plots show *Kcnc1* gene expression in single-cells from CTRL compared to CMS mice. *Kcnc1* is also significantly higher expressed in TST- LHb→DR versus TST- LHb→VTA neurons (see **Figure 7J**), but not different between CTRL LHb→DR versus CTRL LHb→VTA neurons, highlighting that experienced-based classification (CTRL versus CMS) masks transcriptomic correlates of phenotype-based classification (TST- versus TST+) in studying depression.

(D) Regression analysis of differential gene expression between CTRL LHb→VTA (n = 26 cells, 9 mice) versus CMS LHb→VTA (n = 27 cells, 6 mice) neurons and between CTRL LHb→DR (n = 27 cells, 6 mice) versus CTRL LHb→VTA (n = 26 cells, 9 mice) neurons. For each gene, data points represent Log2 (Fold Change) values in both comparisons; colored data points highlight the same genes as identified in panels (A) and (B). This analysis based on experience-based classification revealed less stringent regression and lower statistical significance compared to that based on phenotypic classification (see **Figure 7K**).

(E) Volcano plots show differential gene expression between single LHb→VTA (n = 26 cells, 9 mice) and LHb→DR neurons (n = 18 cells, 6 mice) in CTRL mice. Gold and brown data points denote genes that are significantly enriched in CTRL LHb→VTA versus CTRL LHb→DR neurons, respectively. Highlighted in black are the cell adhesion molecule-coding (CAM; top left), ion channel-coding (top right), transcription factor-coding (bottom left) and synapse-related (bottom right) genes. Highlighted in red are the genes that are detected as significantly differently expressed in LHb→VTA versus LHb→DR neurons from TST- but not from CTRL mice (see **Figures 7H and S7F**). Gray data points represent genes that are not significantly enriched in either category (i.e. absolute value of Log2(Fold Change) < 2 and $p < 0.01$).

(F) Volcano plots show differential gene expression between single LHb→VTA neurons in CTRL (n = 26 cells, 9 mice) versus CMS (n = 27 cells, 6 mice) mice. Green and blue data points denote genes that are significantly enriched in cells from CTRL versus CMS mice, respectively. Highlighted are the cell adhesion molecule-coding (CAM; top left), ion channel-coding (top right), transcription factor-coding (bottom left) and synapse-related (bottom right) genes. Highlighted in red are the genes that are detected as significantly differently expressed in LHb→VTA versus LHb→DR neurons from TST- but not from CTRL mice (see **Figures 7I and S7G**). Gray data points represent genes that are not significantly enriched in either category (i.e. absolute value of Log2(Fold Change) < 2 and $p < 0.01$).

(G) Violin plots show expression of *Ptprr* (top left), *Grik2* (top right), *Lrrtm3* (middle left), *Rundc1* (middle right), Myt1l (bottom left) and *Smim8* (bottom right) as examples from CTRL (n = 26 cells, 9 mice) and CMS LHb→VTA (n = 27 cells, 6 mice) and CTRL LHb→DR (n = 18 cells, 6 mice) mice.

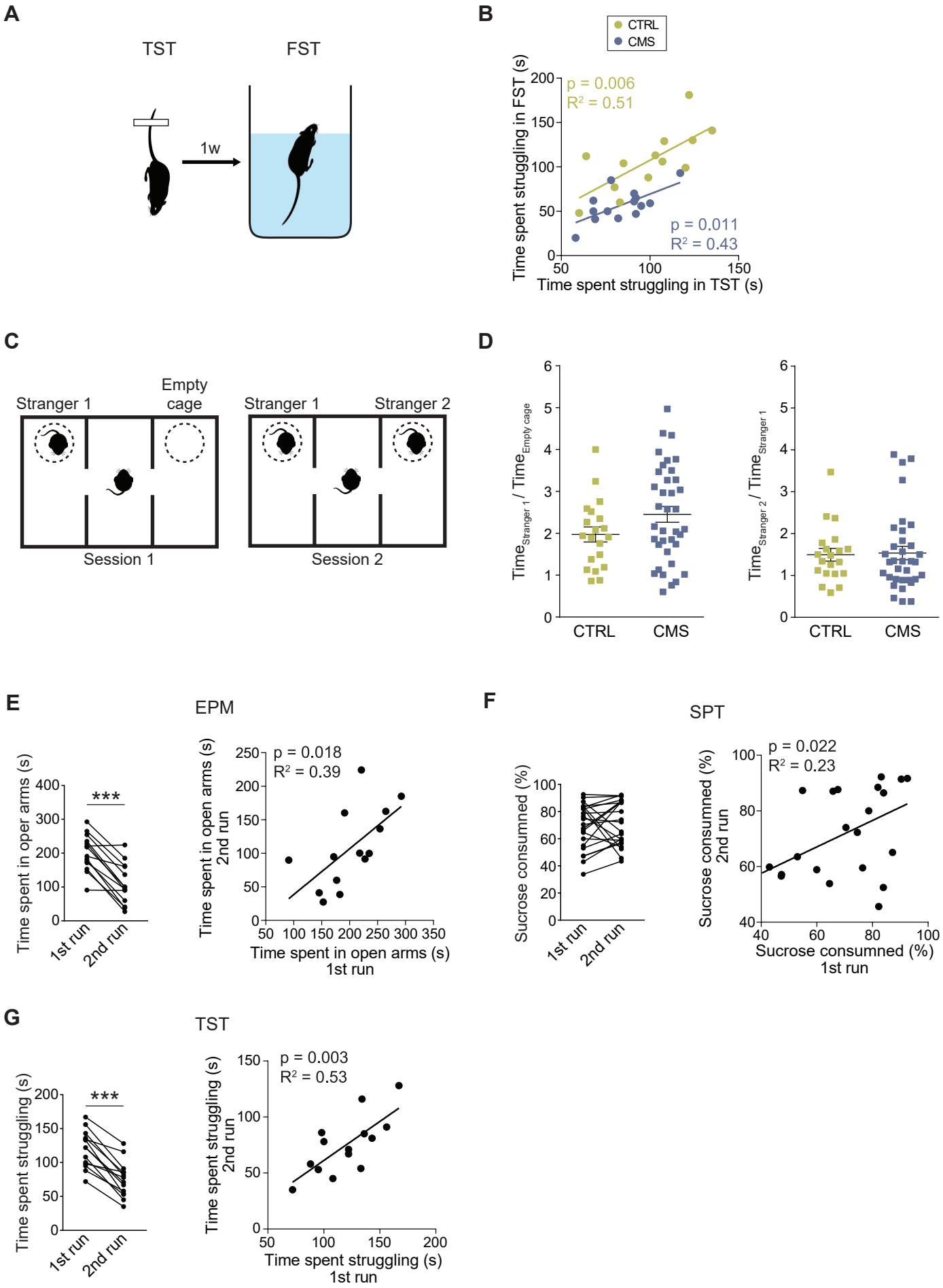
A
TST
FST
1w
B
CTRL
CMS
p = 0.006
R² = 0.51
p = 0.011
R² = 0.43
Time spent struggling in FST (s)
Time spent struggling in TST (s)
C
Stranger 1
Empty cage
Stranger 1
Stranger 2
Session 1
Session 2
D
Time Stranger 1 / Time Empty cage
Time Stranger 2 / Time Stranger 1
CTRL
CMS
CTRL
CMS
E
EPM
Time spent in oper arms (s)
***
1st run
2nd run
p = 0.018
R² = 0.39
Time spent in open arms (s) 2nd run
Time spent in open arms (s) 1st run
F
SPT
Sucrose consumned (%)
1st run
2nd run
p = 0.022
R² = 0.23
Sucrose consumned (%) 2nd run
Sucrose consumned (%) 1st run
G
TST
Time spent struggling (s)
***
1st run
2nd run
p = 0.003
R² = 0.53
Time spent struggling (s) 2nd run
Time spent struggling (s) 1st run

Suppl. Fig. 2 Cerniauskas et al.

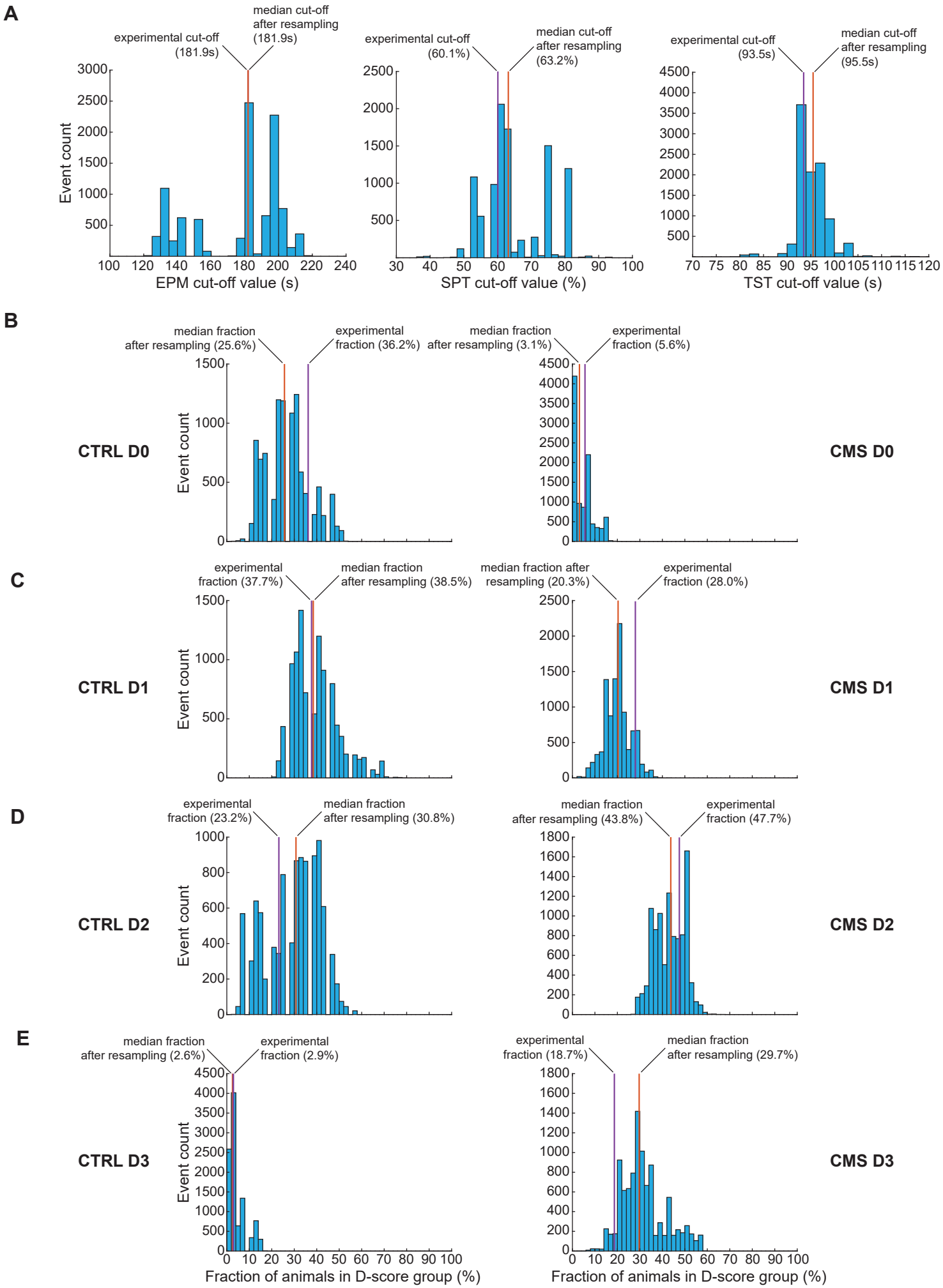

Suppl. Fig. 3 Cerniauskas et al.

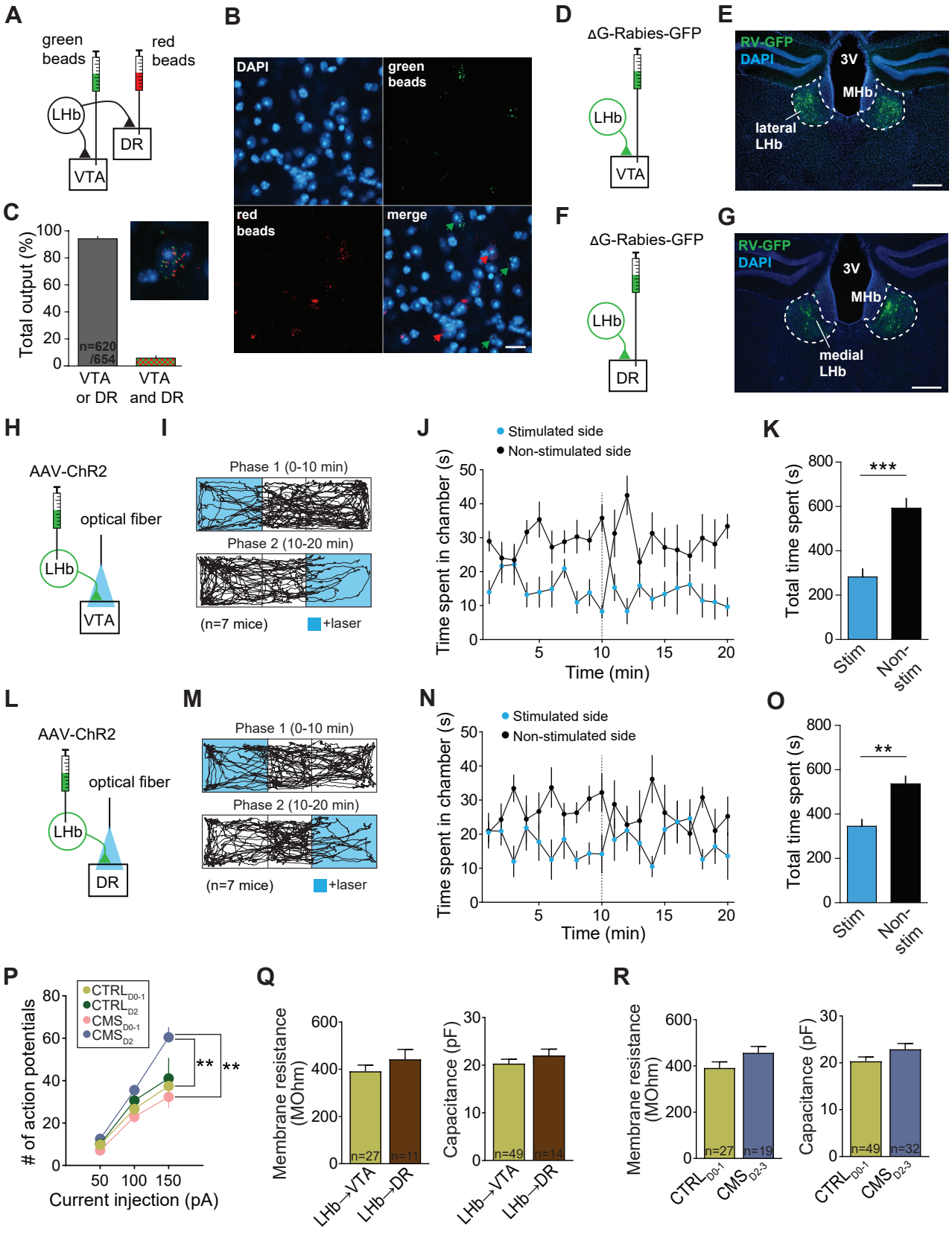

Suppl. Fig. 4 Cerniauskas et al.

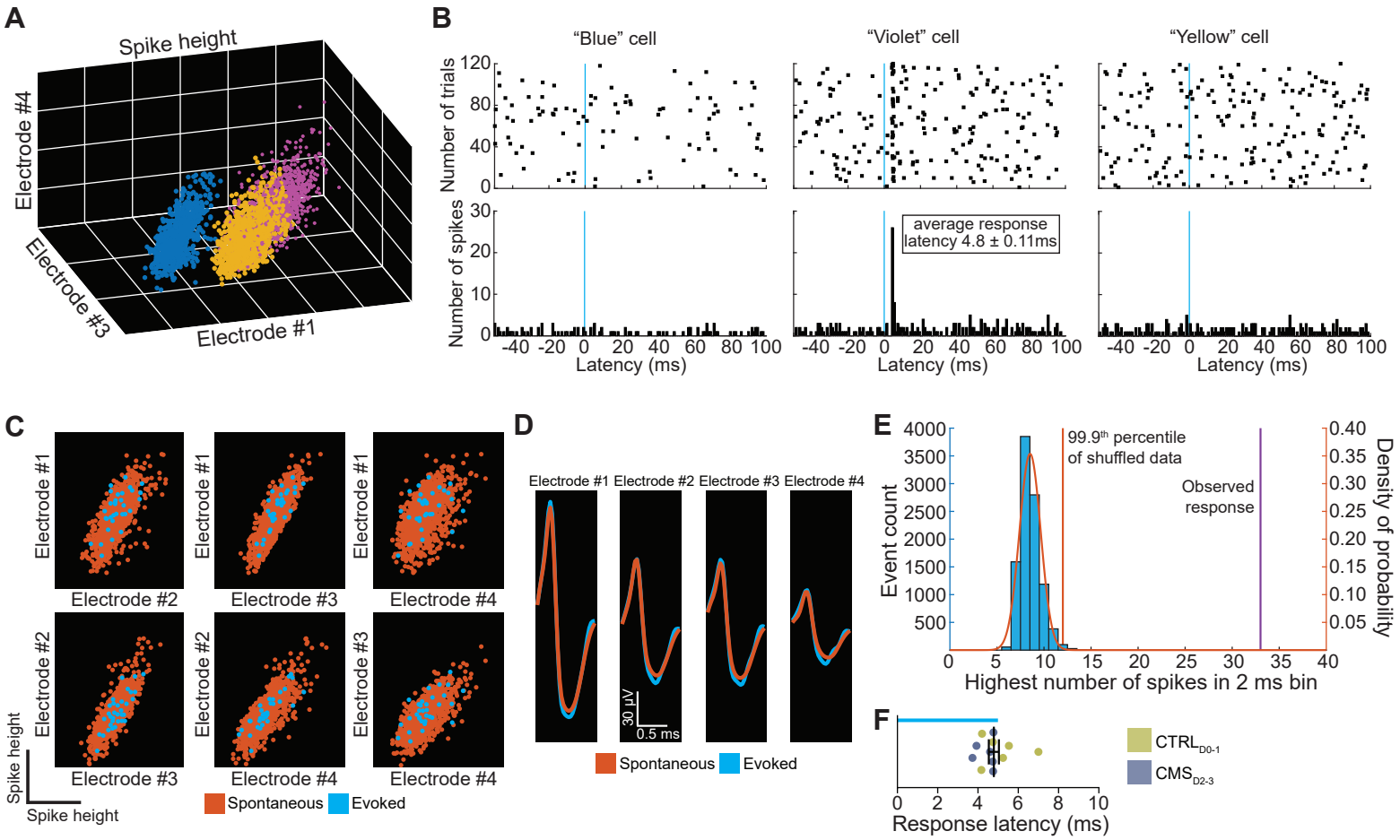

Suppl.Fig.5 Cerniauskas et al.

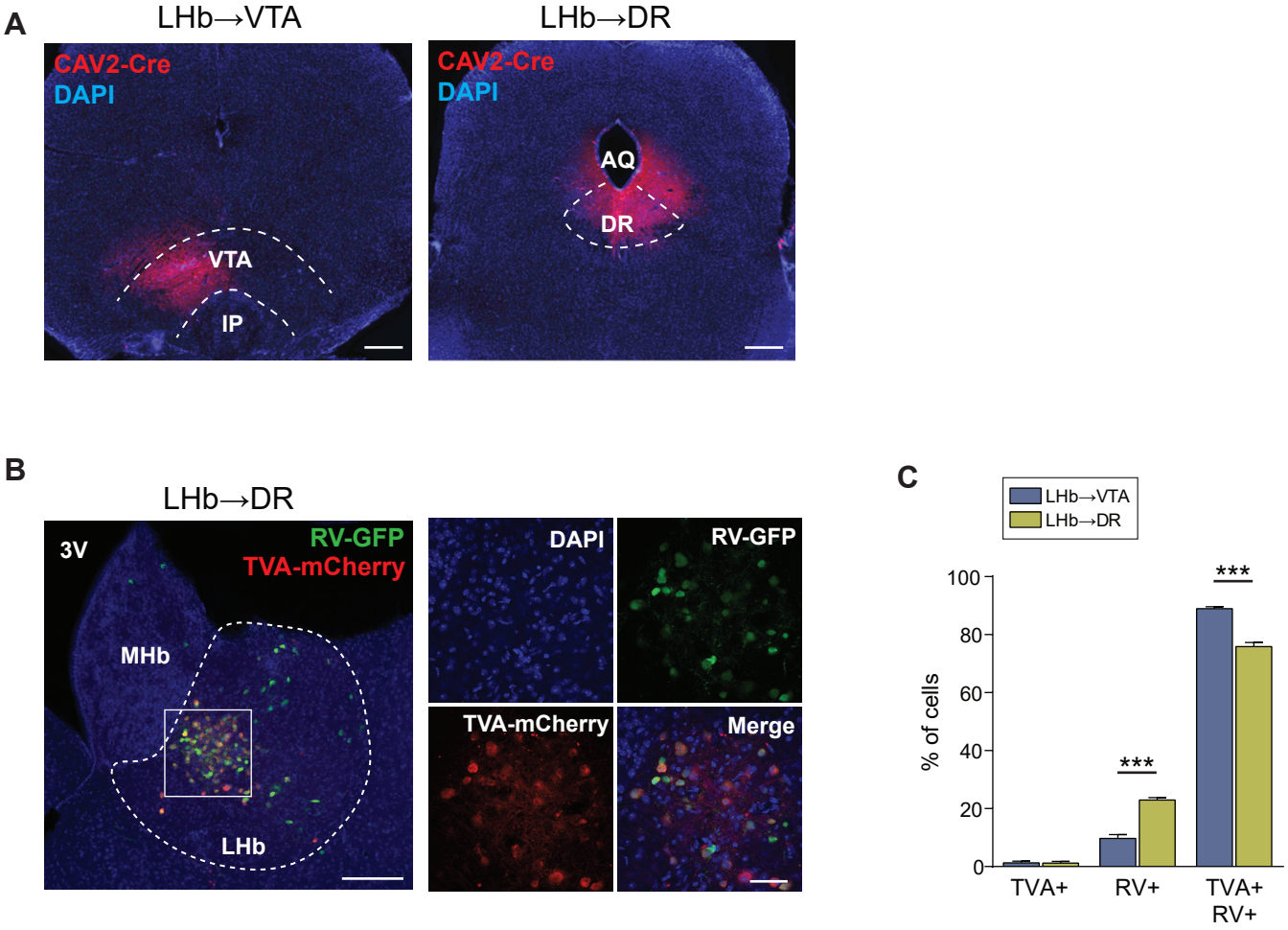

LHb→VTA

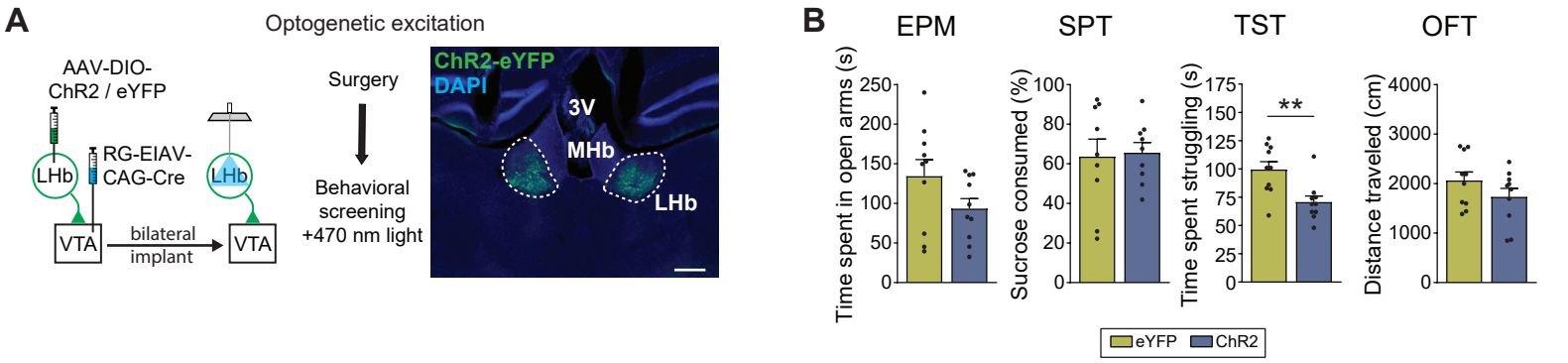

Forced swim test (FST)

LHb→VTA

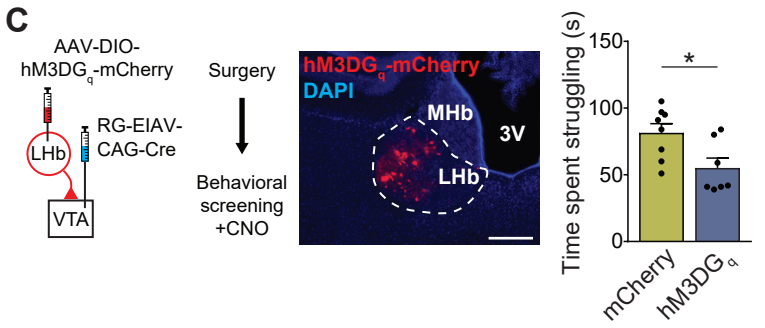

EP→VTA

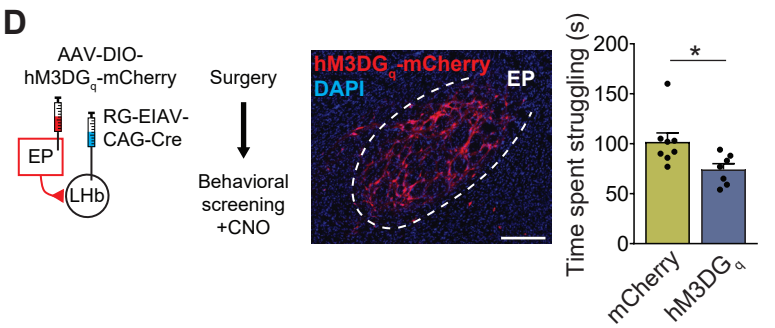

Fixed / progressive ratio tests

LHb→VTA

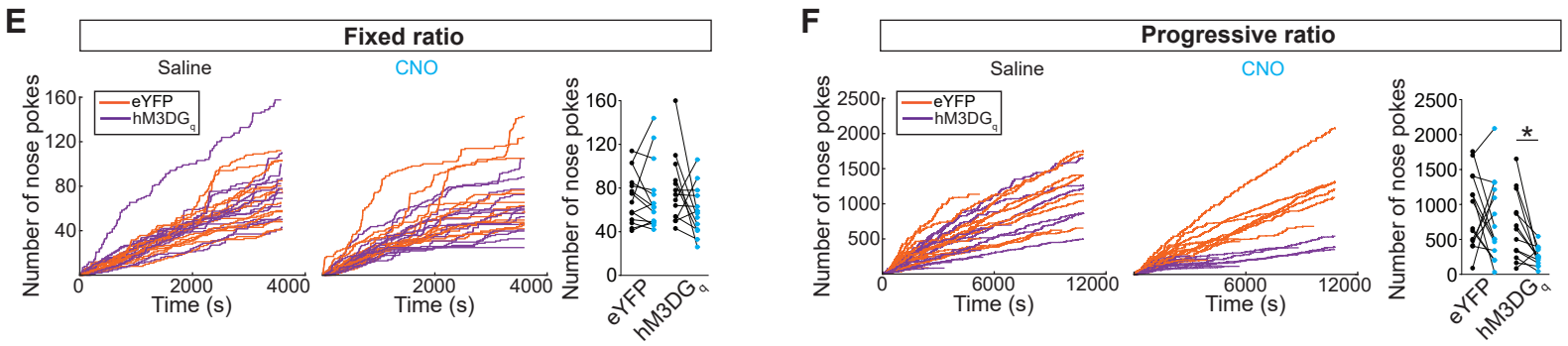

EP→LHb

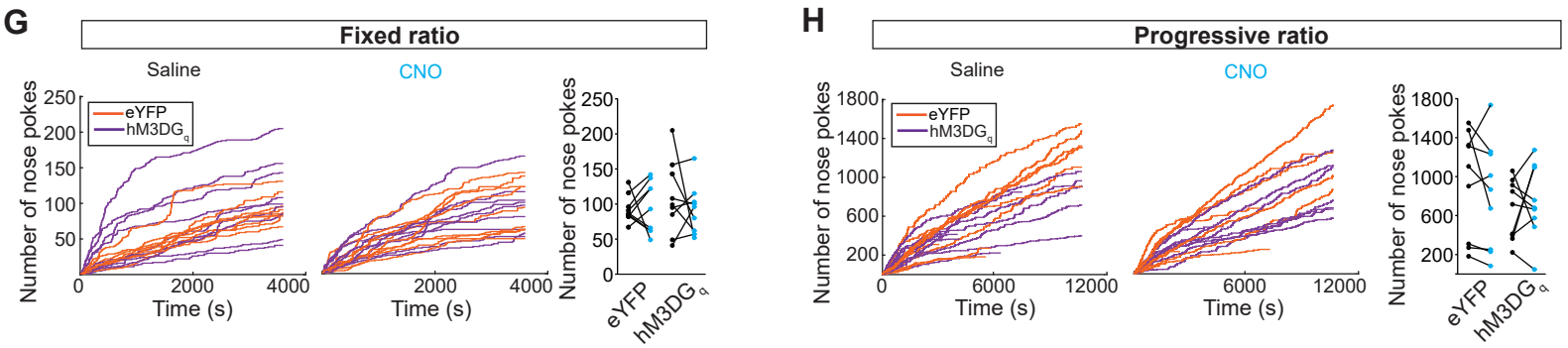

Suppl. Fig. 7 Cerniauskas et al.

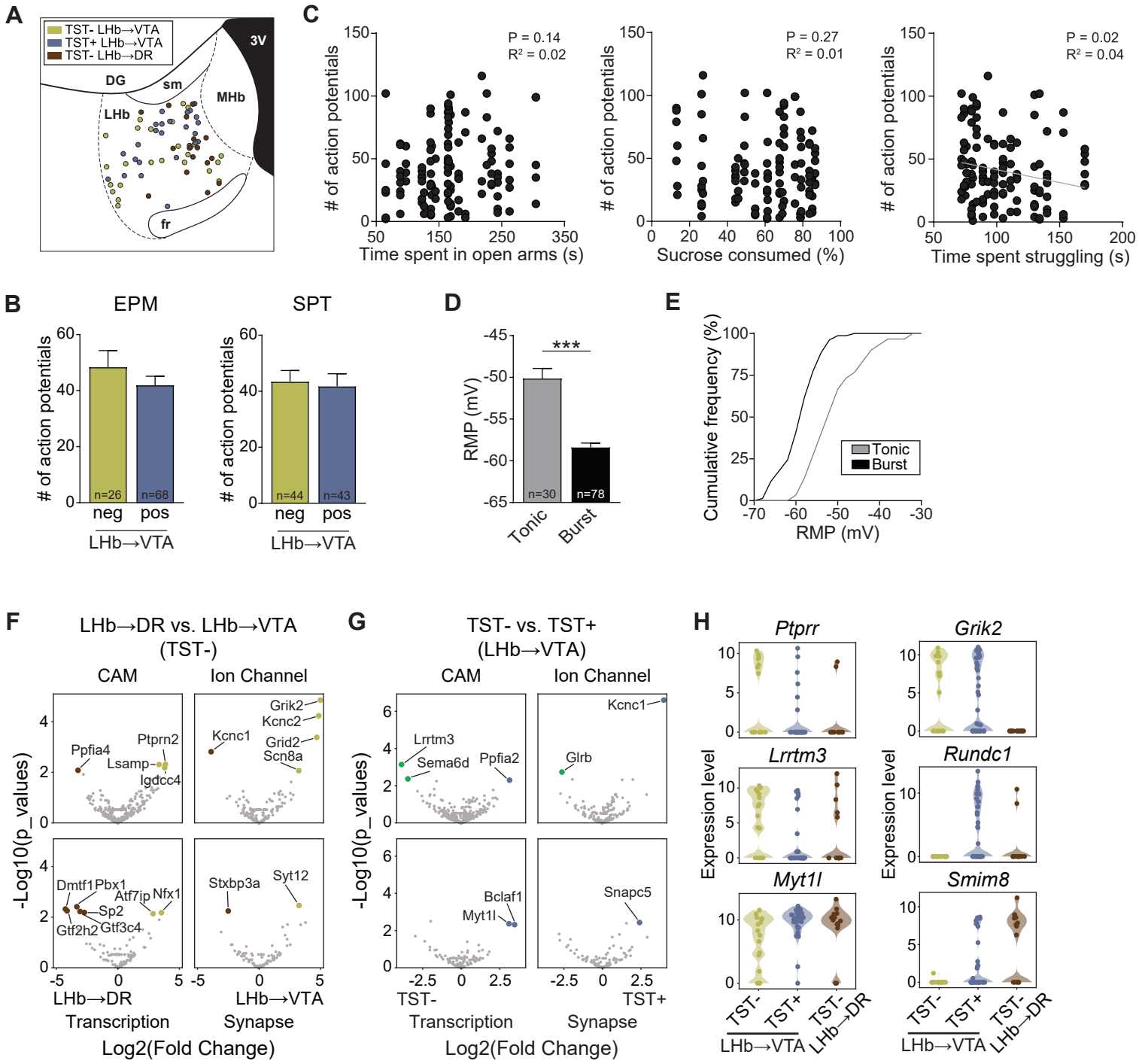

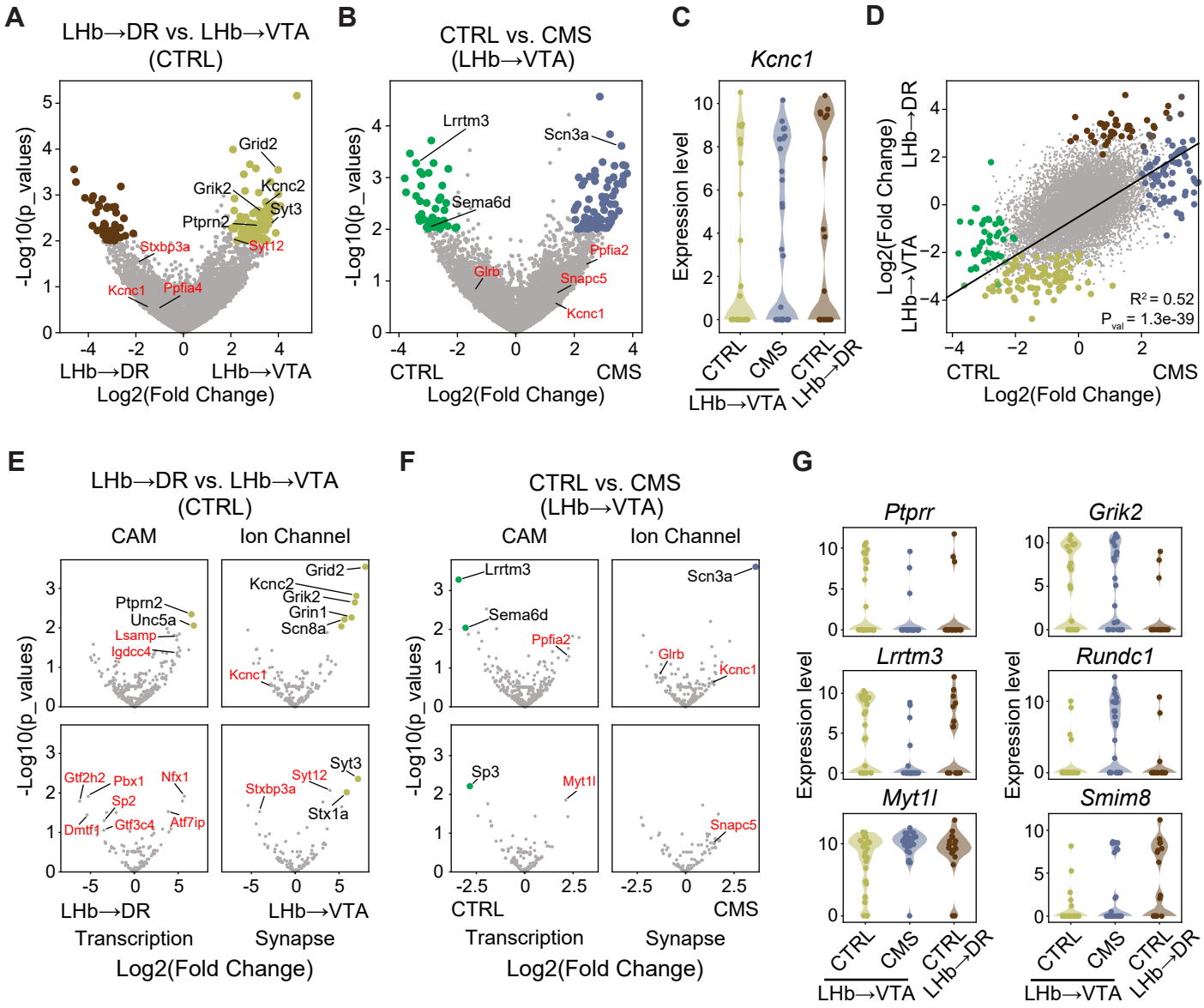
A
LHb→DR vs. LHb→VTA
(CTRL)
-Log10(p_values)
Grid2
Grik2
Kcnc2
Ptprn2
Syt3
Stxbp3a
Syt12
Kcnc1
Ppfia4
LHb→DR
LHb→VTA
Log2(Fold Change)
B
CTRL vs. CMS
(LHb→VTA)
-Log10(p_values)
Lrrtm3
Scn3a
Sema6d
Ppfia2
Glrb
Snapc5
Kcnc1
CTRL
CMS
Log2(Fold Change)
C
Kcnc1
Expression level
CTRL
CMS
CTRL
LHb→DR
LHb→VTA
D
Log2(Fold Change)
LHb→DR
LHb→VTA
R² = 0.52
P_val = 1.3e-39
CTRL
CMS
Log2(Fold Change)
E
LHb→DR vs. LHb→VTA
(CTRL)
CAM
Ion Channel
-Log10(p_values)
Ptprn2
Unc5a
Lsamp
Igdcc4
Grid2
Kcnc2
Grik2
Grin1
Scn8a
Kcnc1
Gtf2h2
Pbx1
Nfx1
Sp2
Dmtf1
Gtf3c4
Atf7ip
Syt3
Syt12
Stxbp3a
Stx1a
LHb→DR
LHb→VTA
Transcription
Synapse
Log2(Fold Change)
F
CTRL vs. CMS
(LHb→VTA)
CAM
Ion Channel
-Log10(p_values)
Lrrtm3
Scn3a
Sema6d
Ppfia2
Glrb
Kcnc1
Sp3
Myt1l
Snapc5
CTRL
CMS
Transcription
Synapse
Log2(Fold Change)
G
Ptprr
Grik2
Lrrtm3
Rundc1
Myt1l
Smim8
Expression level
CTRL
CMS
CTRL
LHb→DR
LHb→VTA

Table S1. Supplemental Data Table

Figure 1A, left panel	CTRL: 195.7 ± 9.4 s, n = 30 mice, CMS: 135.6 ± 5.6 s, n = 70 mice; $p < 0.001$, unpaired Student's t-test
Figure 1B, left panel	CTRL: 73.6 ± 2.5%, n = 33 mice; CMS: 63.3 ± 2%, n = 112 mice; $p < 0.01$, unpaired Student's t-test
Figure 1C, left panel	CTRL: 114.5 ± 3.8 s, n = 43 mice, CMS: 89.6 ± 2.4 s, n = 120 mice; $p < 0.001$, unpaired Student's t-test
Figure 1D	CTRL: n = 69 mice, CMS: n = 107 mice
Figure 1E	EPM: $R^2 = 0.33$, $p < 0.001$, SPT: $R^2 = 0.29$, $p < 0.001$, TST: $R^2 = 0.12$, $p = 0.004$; n = 69 mice, linear correlation
Figure 1F	EPM: $R^2 = 0.19$, $p < 0.001$, SPT: $R^2 = 0.11$, $p < 0.001$, TST: $R^2 = 0.29$, $p < 0.001$; n = 107 mice, linear correlation
Figure 2D	+150 pA: $CTRL_{D0\text{-}1}$: 38.4 ± 3.9 spikes, n = 37 cells (5 mice); $CMS_{D2\text{-}3}$: 50.8 ± 4.3 spikes, n = 38 cells (9 mice); $CMS_{D0\text{-}1}$: 32.3 ± 3.9 spikes, n = 29 cells (5 mice); $CTRL_{D2\text{-}3}$: 43.1 ± 5.8 spikes, n = 28 cells (5 mice); $CTRL_{D0\text{-}1}$ vs. $CMS_{D2\text{-}3}$ $p = 0.022$, $CMS_{D0\text{-}1}$ vs. $CMS_{D2\text{-}3}$ $p = 0.007$, $CTRL_{D2\text{-}3}$ vs. $CMS_{D2\text{-}3}$ $p = 0.64$, $CTRL_{D2\text{-}3}$ vs. $CTRL_{D0\text{-}1}$ $p = 0.66$; two-way ANOVA $p = 0.014$, Sidak's post hoc test
Figure 2E	+150 pA: EPM_{CTRL}: neg: 44.6 ± 6 spikes, n = 23 cells (4 mice), pos: 38.2 ± 4 spikes, n = 42 cells (6 mice), $p = 0.60$; EPM_{CMS}: neg: 45.8 ± 5.9 spikes, n = 24 cells (6 mice), pos: 41.1 ± 4.3 spikes, n = 43 cells (8 mice), $p = 0.76$; two-way ANOVA $p = 0.27$, Sidak's post hoc test;
Figure 2F	+150 pA: SPT_{CTRL}: neg: 38.4 ± 3.9 spikes, n = 37 cells (5 mice), pos: 43.1 ± 5.8 spikes, n = 28 cells (5 mice), $p = 0.99$; SPT_{CMS}: neg: 42.47 ± 4.6 spikes, n = 43 cells (7 mice), pos: 43.5 ± 5 spikes, n = 24 cells (7 mice), $p = 0.99$; two-way ANOVA $p = 0.57$, Sidak's post hoc test;
Figure 2G	+150 pA: TST_{CTRL}: neg: 35 ± 3.6 spikes, n = 42 cells (5 mice), pos: 50.5 ± 6.4 spikes, n = 23 cells (5 mice), $p = 0.052$; TST_{CMS}: neg: 32.3 ± 5.1 spikes, n = 29 cells (5 mice), pos: 50.8 ± 4.3 spikes, n = 38 cells (9 mice), $p = 0.011$; two-way ANOVA $p < 0.001$, Sidak's post hoc test
Figure 2K	+150 pA: $CTRL_{D0\text{-}1}$: 24.7 ± 5.2 spikes, n = 16 cells (3 mice); $CMS_{D2\text{-}3}$: 22.8 ± 5.5 spikes, n = 23 cells (3 mice); $p = 0.81$, unpaired Student's t-test
Figure 2M	Frequency: $CTRL_{D0\text{-}1}$: 2.3 ± 0.4 Hz, n = 11 cells (3 mice); $CMS_{D2\text{-}3}$: 2.8 ± 0.6 Hz, n = 16 cells (3 mice); $p = 0.5$; Amplitude: $CTRL_{D0\text{-}1}$: 33.1 ± 4.1 pA, n = 11 cells (3 mice); $CMS_{D2\text{-}3}$: 27.8 ± 3.1 pA, n = 16 cells (3 mice); $p = 0.3$; both unpaired Student's t-test
Figure 3C	$CTRL_{D0\text{-}1}$: 0.24 ± 0.01 ms, n = 5 cells (3 mice); $CMS_{D2\text{-}3}$: 0.25 ± 0.03 ms, n = 5 cells (3 mice); $p = 0.74$, unpaired Student's t-test
Figure 3D	$CTRL_{D0\text{-}1}$: n = 6 cells (3 mice), $CMS_{D2\text{-}3}$: n = 6 cells (3 mice)
Figure 3E-I	Spikes in bursts: $CTRL_{D0\text{-}1}$: 22.5 ± 1.4%, n = 6 cells (3 mice); $CMS_{D2\text{-}3}$: 27.8 ± 0.9%, n = 6 cells (3 mice); $p = 0.012$; Spikes per burst: $CTRL_{D0\text{-}1}$: 3.5 ± 0.2, n = 6 cells (3 mice); $CMS_{D2\text{-}3}$: 4.8 ± 0.4, n = 6 cells (3 mice); $p = 0.016$; Interburst freq.: $CTRL_{D0\text{-}1}$: 0.4 ± 0.05 Hz, n = 6 cells (3 mice); $CMS_{D2\text{-}3}$: 0.8 ± 0.1 Hz, n = 6 cells (3 mice); $p = 0.004$; Intraburst freq.: $CTRL_{D0\text{-}1}$: 161.3 ± 11.9 Hz, n = 6 cells (3 mice); $CMS_{D2\text{-}3}$: 184.2 ± 22 Hz , n = 6 cells (3 mice); $p = 0.38$; tonic: $CTRL_{D0\text{-}1}$: 4.4 ± 0.6 Hz, n = 6 cells (3 mice); $CMS_{D2\text{-}3}$: 9.9 ± 1.3 Hz , n = 6 cells (3 mice); $p = 0.004$; all unpaired Student's t-test
Figure 3J	$CTRL_{D0\text{-}1}$: 5.8 ± 0.9 Hz, n = 6 cells (3 mice); $CMS_{D2\text{-}3}$: 13.8 ± 1.9 Hz, n = 6 cells (3 mice); $p = 0.003$; unpaired Student's t-test
Figure 4D	EP→LHb→VTA: 13.6 ± 2.9%, EP→LHb→DR: 4.8 ± 0.7%, LH→LHb→VTA: 32 ± 2.5%, LH→LHb→DR: 41.9 ± 2.5%,

Table S1. Supplemental Data Table

Figure 4D, cont.	VTA→LHb→VTA: 6.6 ± 1.6%, VTA→LHb→DR: 13.2 ± 1.4%; VTA: n = 7 mice, DR: n = 6 mice; two-way ANOVA interaction $p < 0.001$; $p < 0.001$ for all three comparisons, Bonferroni post hoc test
Figure 4G	EP: -336.1 ± 81 pA, n = 16/24 cells (67%, 5 mice); VTA: -143.3 ± 18.1 pA, n = 36/45 cells (80%, 9 mice); LH: -907 ± 127.4 pA, n = 14/16 cells (88%, 4 mice); one-way ANOVA $p < 0.001$, LH vs. EP $p = 0.03$, LH vs. VTA $p = 0.009$, EP vs. VTA $p = 0.77$, Tukey's post hoc test
Figure 4H	NMDAR decay time: EP: 36.4 ± 7.8 ms, n = 10 cells (5 mice); VTA: 16.5 ± 4.9 ms, n = 7 cells (5 mice); LH: -102.4 ± 35.7 ms, n = 11 cells (4 mice); one-way ANOVA interaction $p = 0.24$, EP vs. LH $p = 0.03$, VTA vs. LH $p = 0.009$, EP vs. VTA $p = 0.77$, Tukey's post hoc test
Figure 5A	EP: $CTRL_{D0-1}$: 0.44 ± 0.04, n = 12 cells (5 mice); CMS_{D2-3}: 0.26 ± 0.03, n = 13 cells (7 mice); $p = 0.002$; VTA: $CTRL_{D0-1}$: 0.38 ± 0.05, n = 9 cells (6 mice); CMS_{D2-3}: 0.57 ± 0.05, n = 15 cells (7 mice); $p = 0.028$; LH: $CTRL_{D0-1}$: 0.48 ± 0.03, n = 12 cells (4 mice); CMS_{D2-3}: 0.43 ± 0.05, n = 9 cells (6 mice); $p = 0.48$; all unpaired Student's t-test
Figure 5B	EP: $CTRL_{D0-1}$: 4.27 ± 0.8, n = 7 cells (5 mice); CMS_{D2-3}: 10.11 ± 1.6, n = 9 cells (5 mice); $p = 0.009$; VTA: $CTRL_{D0-1}$: 6.8 ± 1.3, n = 11 cells (5 mice); CMS_{D2-3}: 5.57 ± 0.5, n = 9 cells (5 mice); $p = 0.42$; LH: $CTRL_{D0-1}$: 5.86 ± 1.3, n = 9 cells (4 mice); CMS_{D2-3}: 8.80 ± 2.3, n = 11 cells (5 mice); $p = 0.31$; all unpaired Student's t-test
Figure 5C	CTRL no NASPM: n = 5 cells (2 mice), $CTRL_{D0-1}$: n = 5 cells (4 mice), CMS_{D2-3}: n = 8 cells (6 mice); $CTRL_{D0-1}$ vs. CMS_{D2-3}, two-way ANOVA interaction $p = 0.047$
Figure 5F	DR: 13.7 ± 1.2 ms, n = 10 cells (2 mice); VTA: 6.1 ± 0.8 ms, n = 18 cells (5 mice); $p < 0.001$, unpaired Student's t-test
Figure 5G	DR: baseline: 100%, TTX: 2.83 ± 1.5%, TTX+4AP: 0.84 ± 0.6%, n = 7 cells (3 mice); VTA: baseline: 100%, TTX: 5.4 ± 4.6 %, TTX+4AP: 47.6 ± 11.5%, n = 6 cells (3 mice); DR_{TTX} vs. $DR_{TTX+4AP}$ $p = 0.29$, VTA_{TTX} vs. $VTA_{TTX+4AP}$ $p = 0.004$; both paired Student's test
Figure 6B	EPM: eYFP: 172.4 ± 20.3 s, n = 8 mice, hM3DGq: 193 ± 21.2 s, n = 9 mice, $p = 0.5$; SPT: eYFP: 60.8 ± 8%, n = 8 mice, hM3DGq: 53.6 ± 9.9%, n = 7 mice, $p = 0.58$; TST: eYFP: 146.9 ± 7.1 s, n = 9 mice, hM3DGq: 115.1 ± 8.2 s, n = 9 mice, $p = 0.01$; OFT: eYFP: 3787 ± 266 cm, n = 9 mice, hM3DGq: 3566 ± 274 cm, n = 9 mice, $p = 0.57$; all unpaired Student's t-test
Figure 6D	EPM: eYFP: 238.7 ± 13.4 s, n = 10 mice, hM4DGi: 192.2 ± 20.3 s, n = 9 mice, $p = 0.068$; SPT: eYFP: 60.4 ± 8.1%, n = 8 mice, hM4DGi: 71.1 ± 5.4%, n = 8 mice, $p = 0.31$; TST: eYFP: 73.2 ± 2.9 s, n = 10 mice, hM4DGi: 87.4 ± 5.7 s, n = 9 mice, $p = 0.035$; OFT: eYFP: 3703 ± 189 cm, n = 10 mice, hM4DGi: 3508 ± 322 cm, n = 9 mice, $p = 0.6$; all unpaired Student's t-test
Figure 6F	EPM: eYFP: 294.4 ± 17.3 s, n = 7 mice, hM3DGq: 239.1 ± 25.3 s, n = 8 mice, $p = 0.1$; SPT: eYFP: 64.8 ± 7%, n = 7 mice, hM3DGq: 50.8 ± 11.2%, n = 7 mice, $p = 0.31$; TST: eYFP: 106.4 ± 5.1 s, n = 7 mice, hM3DGq: 84.4 ± 7 s, n = 8 mice, $p = 0.027$; OFT: eYFP: 3633 ± 291 cm, n = 7 mice, hM3DGq: 3645 ± 490 cm, n = 8 mice, $p = 0.98$; all unpaired Student's t-test
Figure 6H	EPM: eYFP: 198.5 ± 14.2 s, n = 9 mice, hM4DGi: 227.4 ± 24.8 s, n = 10 mice, $p = 0.34$; SPT: eYFP: 59.8 ± 9.5%, n = 8 mice, hM4DGi: 65.8 ± 9.7%, n = 8 mice, $p = 0.66$; TST: eYFP: 79.9 ± 5.5 s, n = 10 mice, hM4DGi: 107.9 ± 6.4 s, n = 10 mice, $p = 0.004$; OFT: eYFP: 2400 ± 207 cm, n = 10 mice, hM4DGi: 2665 ± 258 cm, n = 10 mice, $p = 0.43$; all unpaired Student's t-test

Table S1. Supplemental Data Table

Figure 7B	TST- VTA: 35 ± 3.6 spikes, n = 42 cells (5 mice); TST+ VTA: 50.7 ± 4 spikes, n = 52 cells (11 mice); TST- DR: 23.5 ± 4.7 spikes, n = 13 cells (3 mice); one-way ANOVA, $p < 0.001$, TST- VTA vs. TST+ VTA $p = 0.011$, TST+ VTA vs. TST- DR $p = 0.003$, TST- VTA vs. TST- DR $p = 0.34$, Tukey's post hoc test
Figure 7F	TST- VTA: -53.8 ± 1.2 mV, n = 42 cells (5 mice); TST+ VTA: -57.1 ± 0.7 mV, n = 53 cells (11 mice); TST- DR: -59.7 ± 1.5 mV, n = 13 cells (3 mice); one-way ANOVA, $p = 0.003$, TST- VTA vs. TST+ VTA, $p = 0.026$, TST- VTA vs. TST- DR, $p = 0.008$, TST+ VTA vs. TST- DR $p = 0.35$, Tukey's post hoc test
Figure 7G	TST- VTA: n = 42 cells (5 mice), TST+ VTA: n = 53 cells (11 mice), TST- DR: n = 13 cells (3 mice)
Figure 7H	LHb→VTA: n = 16 cells (5 mice), LHb→DR: n = 14 cells (5 mice)
Figure 7I	TST- LHb→VTA: n = 16 cells (5 mice), TST+ LHb→VTA: n = 37 cells (10 mice)
Figure 7K	TST- LHb→VTA: n = 16 cells (5 mice), TST+ LHb→VTA: n = 37 cells (10 mice), TST- LHb→DR: n = 14 cells (5 mice)